# The Granular Media Friction Pad: A Novel Biologically-Inspired System for Friction Maximization on a Wide Range of Substrates by Passive Jamming of Granular Material

Dissertation
zur Erlangung des Doktorgrades
der Mathematisch-Naturwissenschaftlichen Fakultät
der Christian-Albrechts-Universität zu Kiel

vorgelegt von

**Halvor Tram Tramsen**

Kiel, 2020

Erster Gutachter: Prof. Dr. Stanislav N. Gorb

Zweiter Gutachter: Prof. Dr.-Ing. Poramate Manoonpong

Tag der mündlichen Prüfung: 21.02.2020

# Contents

# Abstract

Many solutions for getting grip on varying substrates exist in nature and in technical applications, but they fail on substrate geometries they are not specifically designed for. For maximizing friction forces on an unknown substrate, we developed a novel passive load-dependent system that creates high friction forces on a large variety of substrates: The granular media friction pad (GMFP), which consists of a thin elastic membrane encasing loosely filled granular material. When coming into contact with a substrate, the fluid-like granular material flows around the substrate asperities, and large contact areas with the substrate are achieved. Upon applying load, the granular material undergoes the jamming transition, rigidifies and becomes solid-like. High friction forces are generated by mechanical interlocking, internal friction of the granular media as well as by large contact area-mediated friction and deformation of the membrane. This system is able to adapt to a large variety of substrate topologies.

First, we show the friction performance on different substrates and investigate the underlying physical mechanisms in a numerical simulation. We compare the granular media friction pad with bulk silicone samples both in stiffness under different loading conditions as well as for their friction performance on flat and rough substrates and a flat substrate contaminated by large particles.

Then, we investigate the effect of elasticity variation on the generation of friction by varying granular media filling capacity as well as membrane modulus and thickness. The adaptability of the samples is tested by visualizing contact area with large substrate asperities present. Friction performance is evaluated on three different substrate types (flat, rough, contaminated).

Finally, to further increase performance for moist or wet substrates, we adapt the granular media friction pad by structuring the outside of the membrane with a hexagon pattern. The friction performance of the structured and the smooth granular media friction pad is compared on a flat substrate when dry and when completely immersed in mineral oil. The hexagon structuring of the encasing membrane results in a significant increase in friction under lubricated conditions, thus greatly increasing the universal applicability of the granular media friction pad for a multitude of environments.

Overall, the granular media friction pad is able to create high friction on unknown substrate geometries, which makes it suitable for a variety of use cases where stable grip on substrates is important.

# Kurzzusammenfassung

In der Natur und in technischen Anwendungen gibt es viele Lösungen, um festen Halt auf verschiedenen Untergründen zu erzeugen, doch diese versagen auf Untergrundgeometrien, für die sie nicht explizit konzipiert sind. Um Reibkräfte auf unbekannten Untergründen zu maximieren, haben wir ein neuartiges passives Anpressdruck-abhängiges System entwickelt, das auf einer großen Vielfalt von Untergründen hohe Reibkräfte erzeugt: Das Granular Media Friction Pad (Reibkissen mit granularer Materie), das aus einer dünnen elastischen Membran besteht, welche ein locker gefülltes granulares Material umhüllt. Wenn es mit einem Untergrund in Berührung kommt, legt sich das Flüssigkeit-artige granulare Material um die Rauhheiten des Untergrunds herum und erreicht hiermit große Kontaktflächen mit dem Untergrund. Sobald Anpressdruck aufgewandt wird, durchläuft das granulare Material die Jamming-Transition, verfestigt sich und wird Festkörper-artig. Hohe Reibkräfte werden erzeugt durch mechanisches Verhaken, interne Reibung des granularen Mediums sowie große Kontaktflächenabhängige Reibung und Deformation der Membran. Dieses System ist dadurch in der Lage, sich an eine große Vielfalt von Untergrund-Topologien anzupassen.

Zunächst zeigen wir die Reibleistung auf verschiedenen Untergründen und untersuchen die zugrundeliegenden physikalischen Mechanismen in einer numerischen Simulation. Wir vergleichen das Granular Media Friction Pad mit Vollsilikon-Proben bezüglich der Steifheit unter verschiedenen Anpressdrücken sowie ihrer Reibleistung auf flachen und rauhem Untergrund und einem flachen Untergrund, der durch große Partikel verunreinigt ist.

Anschließend untersuchen wir die Auswirkungen von Änderungen in der Elastizität auf die Erzeugung von Reibung, indem wir die Füllkapazität des granularen Mediums sowie den Elastizitätsmodul und die Dicke der Membran variieren. Die Anpassungsfähigkeit der Proben wird untersucht, indem die Kontaktfläche in Anwesenheit von großen Substratrauhheiten visualisiert wird. Zudem wird die Reibleistung auf drei unterschiedlichen Untergrund-Typen (flach, rauh, verunreinigt) bewertet.

Schließlich wird durch Strukturierung der Membran mit einem Hexagon-Profil die Leistung auf feuchten oder nassen Untergründen weiter erhöht. Dabei wird die Reibleistung von strukturiertem und glattem Granular Media Friction Pad auf einem flachen Untergrund in trockenem sowie in vollständig in Mineralöl eingetauchtem Zustand verglichen.

Insgesamt ist das Granular Media Friction Pad in der Lage, hohe Reibkräfte auf unbekannten Untergrundgeometrien zu erzeugen, wodurch es für eine Vielfalt an Anwendungsfällen geeignet ist, bei denen ein fester Halt auf Untergründen wichtig ist.

# Chapter 1

# Introduction

Locomotion often relies on a stable attachment that requires the ability of getting grip by creating high adhesion and friction forces between two surfaces in contact. In biology, two different ways of tackling this challenge are observed: specialized systems for a specific, predictable substrate on the one hand, and generalist systems combining different approaches to cope with a broad variety of substrates, e.g. wet or dry, soft or hard, smooth or rough, on the other [1]. Specialized systems include the head-arresting system of dragonflies [2, 3], wing locking mechanisms in beetles [4], or parasitic louse flies holding onto feathers [5]. These systems feature specifically shaped, highly effective structures, optimized to work with one corresponding substrate but failing in contact with other surfaces. Generalist systems however achieve grip on a diversity of substrates, using a combination of mechanisms each optimized for different substrate types. Typical examples include insects that, during hunt for food, need stable grip on all surfaces to follow their prey. Their feet [2, 6–8] use claws for mechanical interlocking on rough substrates, elongated hair-like structures for attaching to small surface asperities, and spatulae for adhesion on smooth substrates. Another example for the generalist system is the locomotion of snakes, who rely on a combination of muscle-induced local change of stiffness [9], the anisotropy of their scales [9, 10] and the scales' anisotropically microstructured surfaces [11, 12].

In addition, multitudinous animals live in moist or wet environments, but they are still able to get stable grip for secure attachment and locomotion [13]. For a large variety of these animals, we see a common approach to achieve this: Microstructuring their attachment pads [14, 15] with mostly hexagonal arrays of channels, as seen e.g. in a large diversity of frogs [13, 15, 16], in bush crickets [14, 17], stick and leaf insects [18] and salamanders [19, 20].

The microstructure not only helps in spreading mucus as secretory fluid for

enhanced adhesion over the whole attachment pad, but also to remove surplus fluids and enable intimate contact with the substrate [13, 21, 22] when gripping but also while sliding. While microstructuring a surface is highly effective for draining fluids and to enable high friction forces on smooth substrates, a second principle can be observed in nature to conform to wet but also rough substrates to enhance contact area for friction [23]: The microstructured attachment pads feature a complex superstructure resulting in extremely soft attachment pads. This can be done actively [24, 25] or passively by design [13, 17, 21, 23, 26, 27].

Technological applications of adhesion and friction mechanisms mostly specialize on one specific substrate, e.g. hook-and-loop fasteners, or car tires optimized for different environments and conditions, such as high performance tires, road tires or mud tires, tires for different temperatures in summer or winter, for wet or for dry roads. Similarly, robotic systems with optimized foot structures, such as gecko-like structures for climbing flat surfaces [28, 29] or micro spines for climbing rough terrain [30, 31], decrease rapidly in performance and predictability when used in less ideal environments.

For performance under wet conditions, the principle of surface structuring has been adapted in several biomimetic studies both for similar dimensions [14, 15, 20, 32, 33] as well as for much larger structures such as in the tire industry [14, 34–36].

## 1.1 The Granular Media Friction Pad (GMFP)

How would an engineered solution using the generalist approach need to be designed in order to maximize friction forces on unknown substrates, which could be flat, rough, structured or arbitrarily shaped, clean or contaminated, dry or wet?

We developed a novel passive load-dependent jamming system that is able to create high friction forces on a variety of different substrates: the granular media friction pad (GMFP). It consists of a thin elastic membrane encasing a granular material that reversibly undergoes the jamming transition only by varying the normal load of the system. When coming into contact with any kind of substrate, the flexible membrane conforms to the substrate and creates a large real contact area [37]. The granular material encased by the membrane is loosely packed and behaves like a fluid [38, 39], enabling it to conform to the substrate (see figure 1.1a), which results in a minimum of stored elastic deformation energy at the interface to maximize adhesion-mediated friction [37, 40, 41]. Upon applying normal load, the granular material undergoes the jamming transition [42, 43] and becomes solid-like (see figure 1.1b). This results in high friction

forces generated by both the granular material as well as the membrane. The rigidified granular material generates these forces by mechanical interlocking and presumably by energy dissipation due to high friction between the densely packed particles [44–49]. The membrane generates friction forces by the strong deformation of the thin elastic membrane but also by adhesive interaction with the substrate [50, 51]. The combination of normal force pressing the GMFP onto the substrate and the encasing membrane is sufficient for the GMFP to undergo the jamming transition. No active control mechanism such as applying vacuum to induce and control the jamming of the granular material [38, 52–57] is needed. Once the normal load is removed, the granular material returns to a fluid-like state, and so the sample can be removed easily from the substrate without requiring high pull-off forces.

To study this novel friction-enhancing system, we investigate the jamming

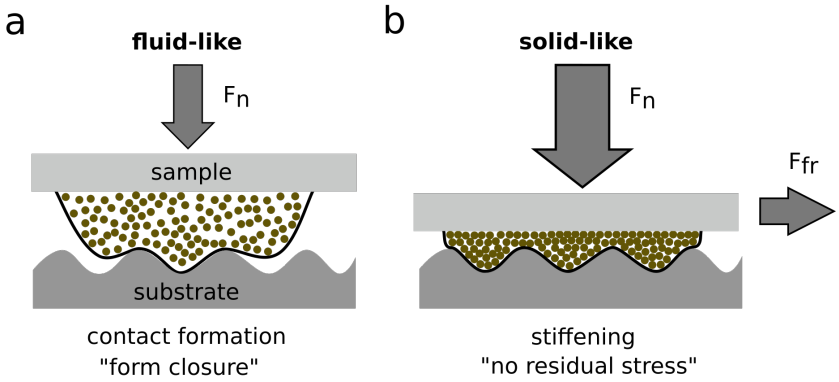


Figure 1.1: Schematic drawing of the granular media friction pad (GMFP): a soft membrane encasing granular material. **a)** Fluid-like behavior when approaching the substrate, **b)** solid-like behavior under normal load $F_n$ resulting in high friction forces $F_{fr}$.

transition of the GMFP. We then characterize its friction coefficient on different clean and contaminated substrates and examine the interplay of the different physical mechanisms by developing a numerical model. To assess the GMFP's performance, we will compare it to two other types of samples made from bulk silicone (see figure 2.1a): a spherical shape resembling the form of an unloaded GMFP, and a 3mm high flat cylinder with the same base area as the GMFP.

## 1.2 Variations of the GMFP

To characterize the friction properties of a system, often the static and the dynamic friction coefficients are used. These two properties describe the relation between normal force acting on the system and resulting friction force from a shearing motion of two contacting bodies. However, it is equally important how the two bodies come into contact and how a structure such as the GMFP adapts to the substrate topography, since this process greatly influences the resulting contact area between the two bodies, the basic requirement for the generation of friction in soft materials. What is more relevant for the generation of friction on any substrate and under any loading condition? The sample being very soft to increase adaptability and contact formation, or the sample being very stiff to increase energy dissipation by the granular media as well as by the deformation of the membrane?

The stiffness of the GMFP is determined by two factors, the granular media and the encasing membrane. For granular media, detailed analyses on the jamming transition and interparticle friction depending on particle type and shape have been conducted [46, 57–61], and knowledge about particle selection for maximizing friction exists. For membrane materials used in granular jamming systems, studies investigating the material's influence on the performance of the system have been conducted [62]. However, regardless of the individual components' properties, frictional systems always have to be examined as a whole. The interplay of components and the resulting properties are as important as the components' properties themselves. How does the filling capacity of the granular media influence the stiffness of the GMFP and the friction coefficient through an earlier onset of granular jamming when densely packed? How does the thickness or the elastic modulus of the membrane change the adaptability to substrate asperities or the amount of energy dissipation during stretching?

To address these questions, we will investigate the effect that changing the GMFP's stiffness has on its friction properties by examining the resulting contact area and the dynamic friction coefficients on three different types of substrates. We will systematically vary the filling capacity and the membrane stiffness. Membrane stiffness can be modified by changing its thickness as well as its elastic modulus. The stiffness of a membrane depends on these parameters by:

$$D = \frac{Et^3}{12(1-\nu^2)} \tag{1.1}$$

with $E$ being the elastic modulus of the membrane, $t$ the thickness of the membrane and $\nu$ the Poisson ratio of the membrane which is considered to be constant for our experiments.

While the GMFP is able to adapt to a large variety of substrate topologies and to form around contaminating particles, this type of structure would probably fail on wet substrates due to its extremely smooth membrane [32, 63, 64] and the resulting hydrodynamic lubrication when sliding over a substrate. To address this, we will structure the membrane with a hexagon pattern. Through this, an increase in friction on wet substrates is expected while maintaining the fluid-like behavior when approaching a rough or contaminated substrate to maximize contact area. We will investigate the friction performance of smooth and hexagonally patterned GMFP on a flat substrate when dry and when completely immersed in mineral oil.

# Chapter 2

# Materials & Methods

In the following, we will describe the samples and substrates employed, the experimental setup as well as our numerical approach for simulating the interplay of the different physical mechanisms during sliding of the GMFP. In total, three different types of experiments are conducted. The first is an introduction of the GMFP including a comparison with two different bulk silicone samples on three different substrates: flat, rough/structured, and contaminated by particles. The second study investigates the effect of membrane elasticity and filling capacity to investigate how these can influence adaptability and friction properties of the GMFP. The last study focuses on membrane structuring for increased performance on wet substrates. For this, a smooth and a patterned GMFP are tested on both dry substrate and when completely immersed in mineral oil.

## 2.1 Samples

First, the granular media friction pad is investigated in comparison with bulk rubber samples of different geometries. In addition, a detailed analysis of membrane stiffness and filling capacity will be conducted. Furthermore, a structuring of the GMFP's membrane for increased performance on wet substrates is undertaken.

### 2.1.1 The Reference GMFP

In general, the GMFP consists of a flexible silicone membrane encasing granular material. To systematically investigate the different components of the GMFP and their interplay, we define a reference GMFP sample.

The reference GMFP consists of a circular silicone membrane (40mm diameter) (Dragon Skin$^{TM}$ 30, Smooth-On, Inc., PA, USA) with a Young's Modulus of

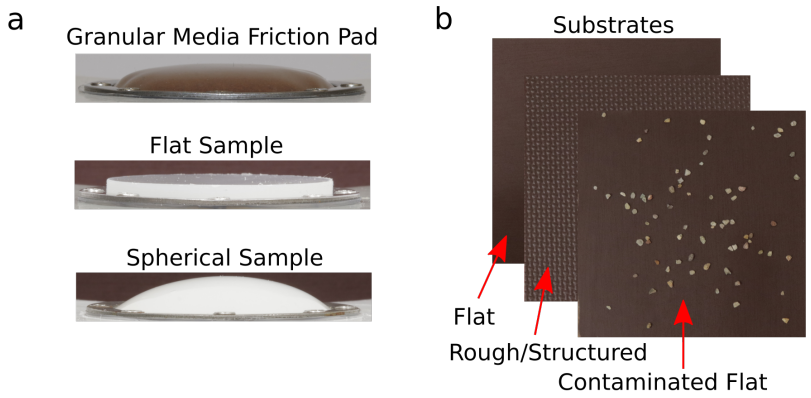


Figure 2.1: **a)** Photographs of the reference GMFP and the two bulk silicone samples (40mm diameter). **b)** Photographs of the three substrates (100mm x 100mm).

$(0.53 \pm 0.02)$MPa. To cast the membrane, uncured resin is poured between two plastic foils fixated on glass plates and separated by three stacked microscope cover slides of 0.15mm height, resulting in a 0.45mm thick silicone membrane. The membrane is then placed flat on a 3D-printed sample holder and screwed down with an adjusting washer (40mm x 50mm x 1mm) using 8 M2 screws. Then, 1.7g of ground coffee (Gold 100% Arabica, Markus Kaffee GmbH & Co. KG, Weyhe, Germany) is pushed behind the membrane through an access hole in the sample holder. The particle size data was obtained by sieving 3 batches of 25g of ground coffee and is given in table 2.1. The ground coffee consists of very rough particles, ideal for mechanical interlocking when pressed against

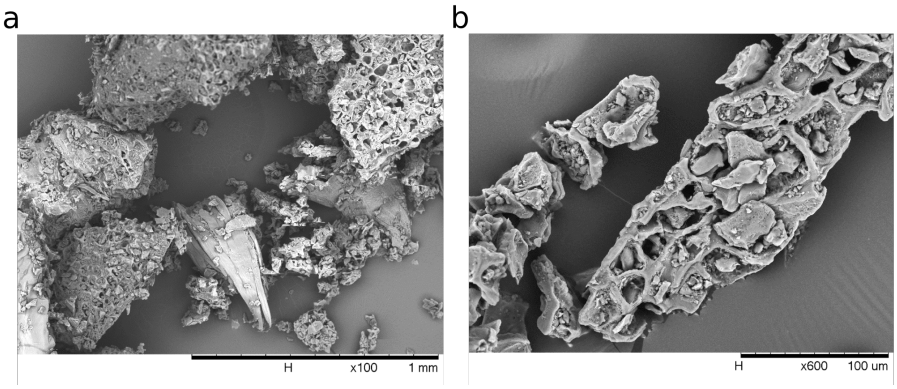


Figure 2.2: SEM images of the ground coffee used as granular material in the GMFP. **a)** 100 times magnification, **b)** 600 times magnification.

each other (see figure 2.2). When the GMFP is filled with 1.7g ground coffee, the volume fraction is $(51 \pm 2)\%$.

| sieve size [$\mu$m] | mass [%] |
|---|---|
| $< 125$ | $0 \pm 0$ |
| 125 | $1.5 \pm 2$ |
| 250 | $46.6 \pm 3$ |
| 500 | $50.5 \pm 4$ |
| 1000 | $1.4 \pm 1$ |
| 2000 | $0 \pm 0$ |

Table 2.1: Granular media (ground coffee) particle sizes.

### 2.1.2 Comparison with Bulk Silicone

For comparison with the reference GMFP, in addition, two other types of samples are cast from bulk silicone also made from Dragon Skin$^{\text{TM}}$ 30 (see figure 2.1a): A sample with a spherical shape to represent the reference GMFP in the unloaded state and a flat cylinder with 3mm height and the same base area as the GMFP as defined by the inner circumference of the adjusting washer. For this test, all three sample types are produced four times and each sample is tested on three different substrate types (flat, rough/structured and contaminated by gravel particles) in random order.

### 2.1.3 Membrane and Filling Capacity Variations

To investigate the effect of membrane elasticity and filling capacity, one of the following parameters of the reference GMFP is varied at a time in each subset of experiments of our second study:

- filling capacity (1g, 1.7g, 2.7g, 3.7g)
- membrane thickness (0.15mm, 0.45mm, 1mm, 2mm)
- membrane modulus (Dragon Skin$^{\text{TM}}$ 10 with $(0.16 \pm 0.01)$MPa, Dragon Skin$^{\text{TM}}$ 20 with $(0.33 \pm 0.01)$MPa and Dragon Skin$^{\text{TM}}$ 30 with $(0.53 \pm 0.02)$MPa.)

All sample types are produced four times and each sample is tested for all normal loads on three different substrate types (flat, rough/structured and contaminated by gravel particles) in random order.

### 2.1.4 Hexagon Structuring

To investigate friction properties on wet substrates, two different types of GMFP are investigated: one with a smooth membrane (see figure 2.3a) and one with a hexagon patterned membrane (see figure 2.3b). In contrast to the reference

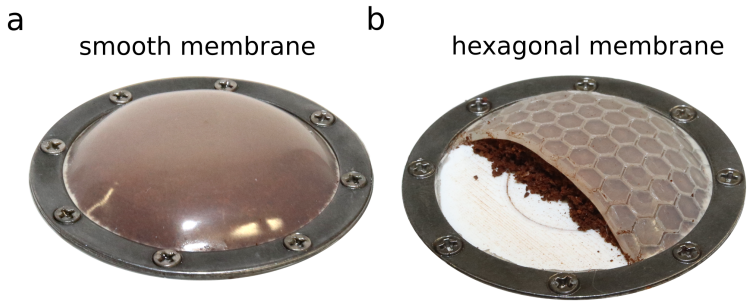


Figure 2.3: **a)** Photograph of a GMFP with a smooth membrane. **b)** Photograph of a GMFP with a hexagonally patterned membrane; the membrane is cut open, showing the GMFP's ground coffee filling.

GMFP, the Dragon Skin$^{TM}$ 30 membrane is cast into a 1mm thick membrane. For the hexagon membrane, a hexagon grid with 2.19mm circumcircle, 0.4mm groove width and 0.6mm groove depth is 3d printed from PLA using an Original Prusa i3 Mk3 (Prusa Research s.r.o., Prague, Czech Republic). The grid is glued onto one of the plastic foils before moulding the membrane in the same way as the smooth membrane. Thus, the tops of the resulting hexagonal pillars have the same surface properties as the smooth membrane. To examine the effect of membrane structuring on the friction performance of the GMFP under dry and under lubricated conditions, both the smooth and the hexagon patterned GMFP are produced 12 times and tested subsequently on a dry substrate and on an oily substrate. For each sample and substrate combination, friction measurements are conducted at four different normal loads ranging from the sample weight itself (1N) up to a maximum normal load of 19.36N.

## 2.2 Substrates

The substrates were chosen to represent a wide variety of surfaces and conditions by using a flat and a rough/structured surface that can subsequently be contaminated by either gravel particles or mineral oil.

The flat substrate consists of the flat side of wire mesh plywood ($R_a = 3.6\mu m$). For the rough/structured substrate, the structured side of wire mesh plywood ($R_a = 50.9\mu m$) was selected (see figure 2.1b).

For visualizing contact area, the wire mesh plywood can be replaced by an acrylic glass plate to enable a live view of the GMFP through the substrate.

### 2.2.1 Gravel Particle Contamination

To represent large particle contamination (up to half the height of the reference GMFP), 0.5g of 1-2mm gravel particles (see figure 2.1b) are placed onto the flat wire mesh plywood. This is done to investigate the adaptability of the GMFP to large asperities as well as the effect of third body contamination on the friction properties of the GMFP.

### 2.2.2 Mineral Oil Contamination

To measure the friction on both dry substrate and submerged under mineral oil we place a small wall around the substrate. Mineral oil (Mineral oil 330779, Sigma-Aldrich Chemie GmbH, Taufkirchen, Germany) is poured onto the substrate with a depth of at least 3mm to fully submerge the contact area between GMFP and substrate.

### 2.2.3 Visualization of Contact Area

To investigate the GMFP's adaptability to conform around a large substrate asperity, a glass sphere (2.5mm diameter) is placed onto a smooth glass substrate. The sample is lowered onto the substrate and loaded with the respective normal load $F_n$. Contact area is visualized using total internal reflection. For each normal load, the sample is completely lifted off the substrate and the glass sphere repositioned. Normal load ranges from the sample weight itself (1N) up to a maximum of 112.09N.

## 2.3 Experimental Setup

The experimental setup consists of vertical and horizontal shafts with freely running linear bearings holding substrate and sample (see figure 2.4). The substrate is pulled horizontally at 1mm/s for 50mm using a linear testing machine (Xforce HP 500N, ZwickiLine, Zwick Roell, Ulm, Germany) that measures the pulling force. The sample can move vertically above the substrate while the substrate is slid sideways underneath. Additional weights can be placed on the sample to increase normal load during the experiment. The friction generated by the experimental setup itself does not exceed 0.2N under all loading conditions, and

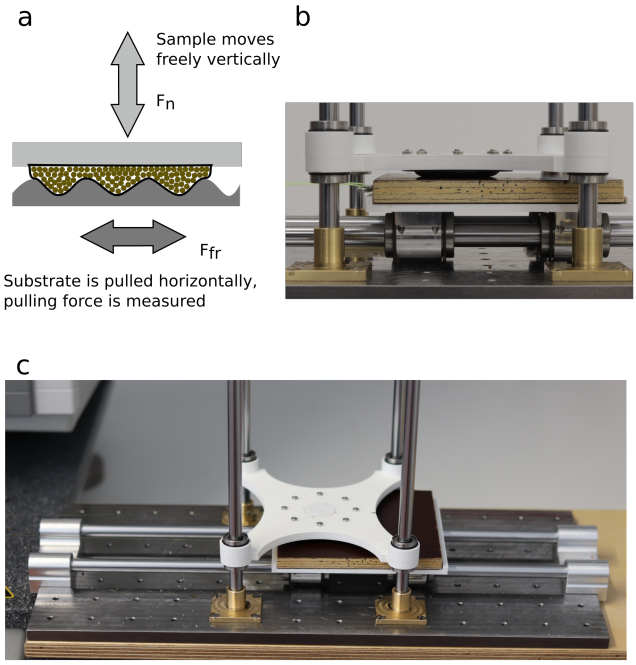


Figure 2.4: Experimental setup. **a)** Schematic illustration of acting forces. **b)** Side view of the setup. **c)** Top view of the experimental setup.

due to the much higher friction forces caused by the GMFP and the other samples, this is considered negligible for the discussion of the results. For obtaining the sliding friction force, the pulling force is averaged for 10s, 35s after sliding starts (see gray area in figure 3.2). To achieve precise and reliable results, the sample holder needs to be sufficiently mobile while being lightweight to examine a mostly uncompressed GMFP (total weight including bearings 1N), but also sufficiently strong to withstand high friction forces at high normal loads. Thus, a small torsion at higher loads can be observed (see supplementary Video_S4) but is very small compared to the total deformation of the GMFP.

## 2.4 Numerical Simulation

In the numerical simulation, the granular particles ($N = 200$) are modeled by a Gaussian repulsion $F_{rep} = G \exp -[(x_k - x_{k'})^2 + (y_k - y_{k'})^2]/r_i^2]$ with effective interaction radius $r_i = r_{02}$ for particle - particle repulsion and $r_i = r_{01}$ for particle - membrane repulsion. The elastic membrane is modeled by single points ($N = 200$) connected by springs with anisotropic elastic constants. The membrane connects to the sample holder at both ends and membrane and particle properties are adjusted to obtain the best coincidence between equilibrium

shape of the membrane and its form in the physical experiment. After an initiation period, the modelled GMFP is pulled over a flat substrate at a constant normal load (see figure 2.5, where the initiation period and a typical simulation run are depicted). Friction is modeled by energy dissipation due to velocity $\nu_j$

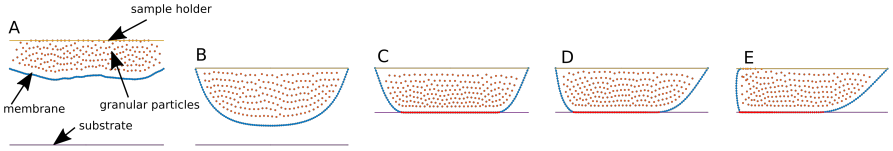


Figure 2.5: Illustration of the initiation period of the numerically simulated GMFP (**A-C**) and a typical simulation run (**D-E**). The sample is filled by an initial random distribution of particles above the unstretched membrane. The sample holder is moved downwards, pushing the particles against the elastic membrane (**A**) until the sample holder touches the ends of the membrane and the granular media friction pad can dynamically relax to its base state (**B**). The GMFP is loaded by moving the substrate upwards and ends in an equilibrium, which is determined by the balance of all internal forces of the system and its external load (**C**). Then, horizontal sliding starts (**D**) and the GMFP deforms (**E**).

dependent forces $F = \eta_i(\nu_1 - \nu_2)$ with tunable friction $\eta_i$ for particle - particle, particle - membrane and particle - sample holder interaction. Friction forces at the contact area between membrane and substrate are modeled as dry friction, where motion is initiated after a critical force threshold $F_{eff}$ is exceeded. This force threshold consists of a material-dependent constant $F_0$ and an adhesion-dependent component increasing with contact time $\tau_j$, resulting in an effective threshold force of $F_{eff} = F_0 \left[1 + B_1\tau_j / \left(1 + B_2\tau_j\right)\right]$, which is proportional to the time $\tau_j$ at short timescale and saturates after a while, with the time defining constants $B_1$ and $B_2$.

# Chapter 3

# Results & Discussion

In the following, we will examine and discuss the results of our experiments with the GMFP.

## 3.1 Reference Granular Media Friction Pad

To study the reference GMFP, we investigated the jamming transition of the GMFP. We then characterized its friction coefficient on different clean and contaminated substrates and examined the interplay of the different physical mechanisms by developing a numerical model. To assess the GMFP's performance, we compared it to two other types of samples made from bulk silicone (see figure 2.1a): a spherical shape resembling the form of an unloaded GMFP, and a 3mm high flat cylinder with the same base area as the GMFP.

### 3.1.1 Jamming Transition

To demonstrate the GMFP's jamming behavior, the stiffness of the samples was obtained from the slope of the force-displacement curves for different normal loads (see figure 3.1a). In the first few seconds of the experiment, the force curve of the GMFP exhibits a distinct initial linear slope before flattening. Here, the forces resulting from the small deformation of the membrane are considered to be negligible [62] in comparison to the forces generated by the granular material (see supplementary Video_S1). This linear part, which can differ in duration depending on the normal load, is fitted and the resulting slope is shown in figure 3.1b, clearly showing the GMFP's jamming transition [42, 57, 65]. The increase in normal load in combination with the deformation of the encasing membrane is sufficient for the particles to undergo the jamming transition without needing

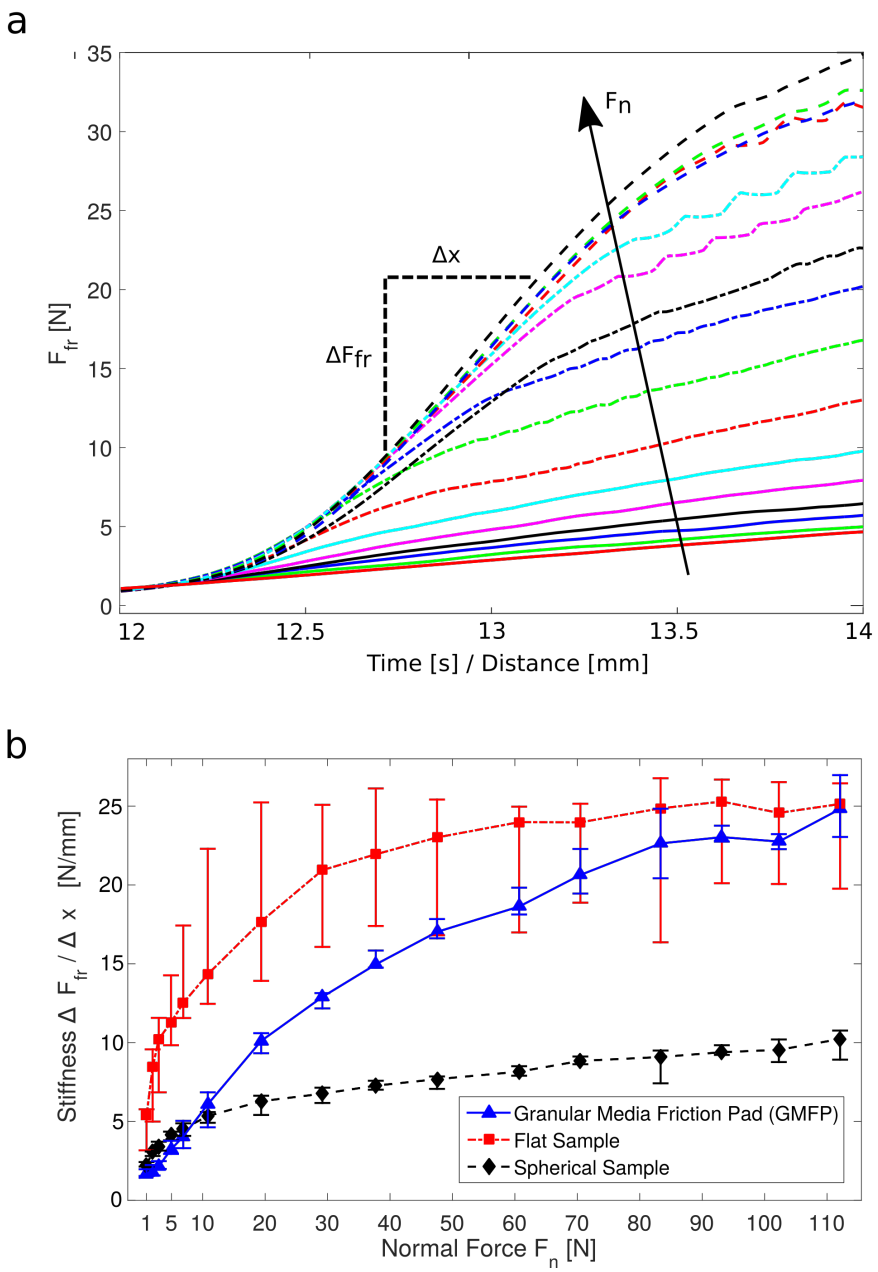


Figure 3.1: **a)** Slope of the force curve $F_{fr}$ at the beginning of the experiment. Normal load $F_n$ ranges from the sample weight (1N) up to the maximum load of 112.09N. **b)** Initial stiffness of the samples showing the jamming transition of the GMFP from very soft to stiff, the data points showing the median, the error bars showing the minimum and maximum values.

outside forces e.g. vacuum [38, 52] or surrounding solid walls [43]. For low normal loads $F_n$, the GMFP is the softest of the three samples, while at high $F_n$, the

GMFP's stiffness is comparable to the flat bulk silicone sample. The spherical sample is rather soft under all normal loads since its elongated shape facilitates bending more than the flat sample of the same material. For the flat sample, a high stiffness even at low load was expected. The opposite was observed since initial strain due to fixation of the sample resulted in small and unstable contact areas at low normal loads. The spherical sample and the GMFP did not exhibit this behavior, since they are much less prone to strain by design.

### 3.1.2 Friction Measurements

An exemplary friction curve of a GMFP on a clean flat substrate at a normal load $F_n = 19.36$N is shown in figure 3.2. The friction behavior consists of four regimes: First, only the jammed granular particles are sheared, leading to a steep incline (A). Then, in addition to the shearing of the particles, the flexible membrane is being stretched, leading to a low incline in friction force $F_r$ (B). (C) marks the point of the transition from static friction to global dynamic friction (D). Upon removing shear and normal load from the system, the membrane's strain causes the GMFP to mostly relax to its initial configuration. To obtain the dynamic friction forces, 10s of the sliding force were averaged (gray area in figure 3.2).

The results of the friction experiments on all substrates are shown in figure 3.3. At $F_n = 19.36$N, resulting friction forces on the clean flat substrate exceed $F_r > 35$N (see left column of figure 3.3a) and are of the same order as forces that universal grippers using granular jamming in combination with active vacuum switching can achieve (see e.g. supplementary information for [38], where a gripper bag with a radius 4.3cm is pulled over a test sphere achieving maximum

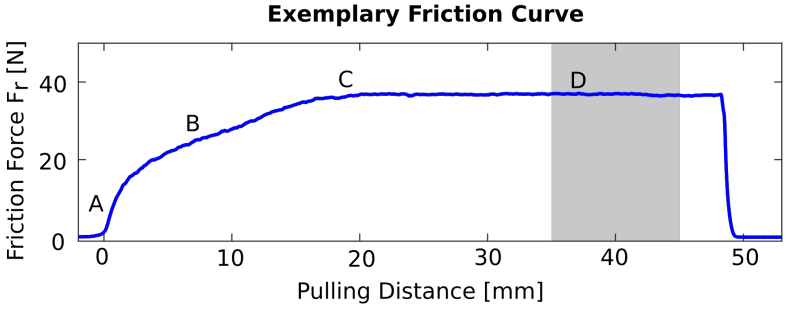


Figure 3.2: Exemplary friction curve showing the phases of the pulling curve at $F_n = 19.36$N: A) shearing of granular material, B) shearing of granular material and elastic deformation of membrane, C) static friction peak, D) dynamic friction.

friction forces of $F_r \approx 34N$ with a similar contact area as the GMFP).

**Flat Substrate**

On the flat substrate (see figure 3.3a), the GMFP exhibits extremely high friction forces at low normal load. This can be attributed to the high adhesion forces of the GMFP's flexible membrane [40, 66]. While the flat silicone sample would be expected to perform equally well, the minimal stress caused by the fixation of the sample onto the sample holder leads to a slight deformation of the flat silicone. The sample's own weight cannot sufficiently flatten the sample to create a larger contact area for adhesion-mediated friction. The spherical sample cannot achieve large contact areas under any loading conditions, thus achieving lower friction forces than the other two samples for all normal loads. The GMFP shows a much later onset of sliding friction compared to the bulk silicone samples. Also it deforms strongly before sliding begins (see supplementary Video_S2), while still being able to create large contact areas during sliding (see supplementary Video_S3).

**Structured Substrate**

On the structured substrate (see figure 3.3b), friction forces are generally lower since contact area between sample and substrate is reduced due to surface corrugations and higher roughness of the substrate. Nevertheless, the GMFP achieves highest friction coefficients for all normal loads due to its adaptability at contact formation and deformability during sliding [53, 54].

**Contaminated Flat Substrate**

On the flat substrate contaminated by large particles (see figure 3.3c), the flat and spherical samples exhibit very low friction, which is mostly dominated by third body friction due to the rolling gravel between sample and substrate. The GMFP's performance is entirely different, greatly exceeding that of the bulk silicone samples. The sliding of the GMFP over the contaminated substrate as well as a visualization of the contact area of the GMFP on a similarly contaminated acrylic glass substrate is shown in figure 3.4. This can also bee seen in the supplementary Video_S4 and Video_S5. At low normal forces, the elastic membrane's tension is so high that it only lies atop the contaminating particles without yet reaching the substrate. At higher normal loads, the granular media push the membrane around the particles, creating large contact areas and a high friction coefficient. In comparison to the rubber bulk samples, the thin elastic membrane requires much less force to squeeze around the particles and

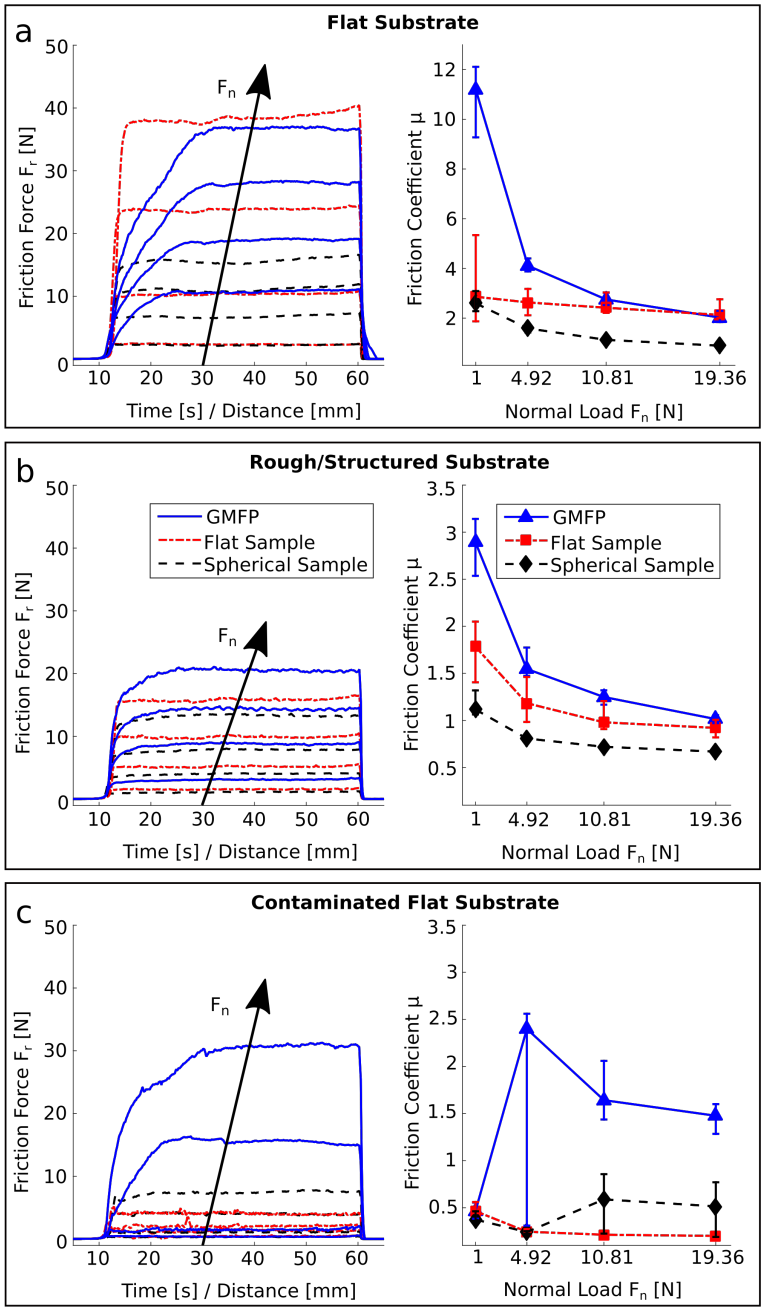


Figure 3.3: Friction performance (left column) and resulting friction coefficients (right column) of the reference GMFP as well as the two bulk silicone samples on **a)** the flat substrate, **b)** the rough/structured substrate and **c)** the contaminated flat substrate.

to get in contact with the substrate even at lower normal forces [37]. This high adaptability resulting from the membrane as well as the granular material [52]

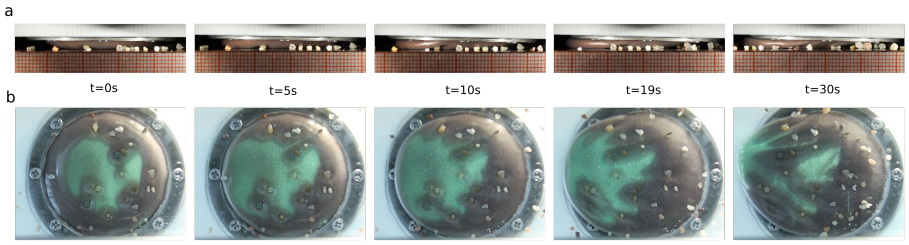


Figure 3.4: Sliding of the GMFP **a)** at 19.36N over contaminated flat substrate **b)** at 10.81N over similarly contaminated acrylic glass. Contact area is lit up in green.

enables the GMFP to achieve high friction forces although the contaminating particles are half the size of the GMFP's height.

### 3.1.3 Numerical Model

In addition to the experiments, we newly developed a numerical 2-dimensional model. This minimalistic but realistic model is used to describe how the occurring friction forces are composed of forces stemming from the granular material as well as from the elastic membrane. This can be seen in figure 3.5, where the total friction force (figure 3.5a) results from the addition of the forces generated by the membrane (figure 3.5b) and of the forces generated in the granular material (figure 3.5c). As can be seen, at the beginning of the experiment, friction forces generated by the granular media clearly dominate the friction properties of the GMFP. Only after a longer sliding distance, friction forces from the deformation of the membrane contribute to the total friction force, thus clearly showing the relevance of the rigidified granular material to the total friction properties of the GMFP. The range of normal load shown here ranges from the GMFP just touching the substrate to the highest compression numerically and physically reasonable, where the effect of rigidification of the granular material is clearly visible from the strong increase of the slope at the beginning of the force curve in figure 3.5c similar to the change in slope of the force curve seen in figure 3.1a.

To visualize the contact dynamics of the GMFP when sliding on a substrate, the motion of the sample when sliding is plotted in figure 3.5d. Here, the green outer area displays the motion of the GMFP over time. Static contact of the elastic membrane on the substrate is displayed in yellow, dynamic sliding contact in blue. We distinguish between static and dynamic by time-dependent adhesion. When the membrane stays longer in contact with the substrate, the color transitions from blue to yellow, thus indicating a long static contact. When

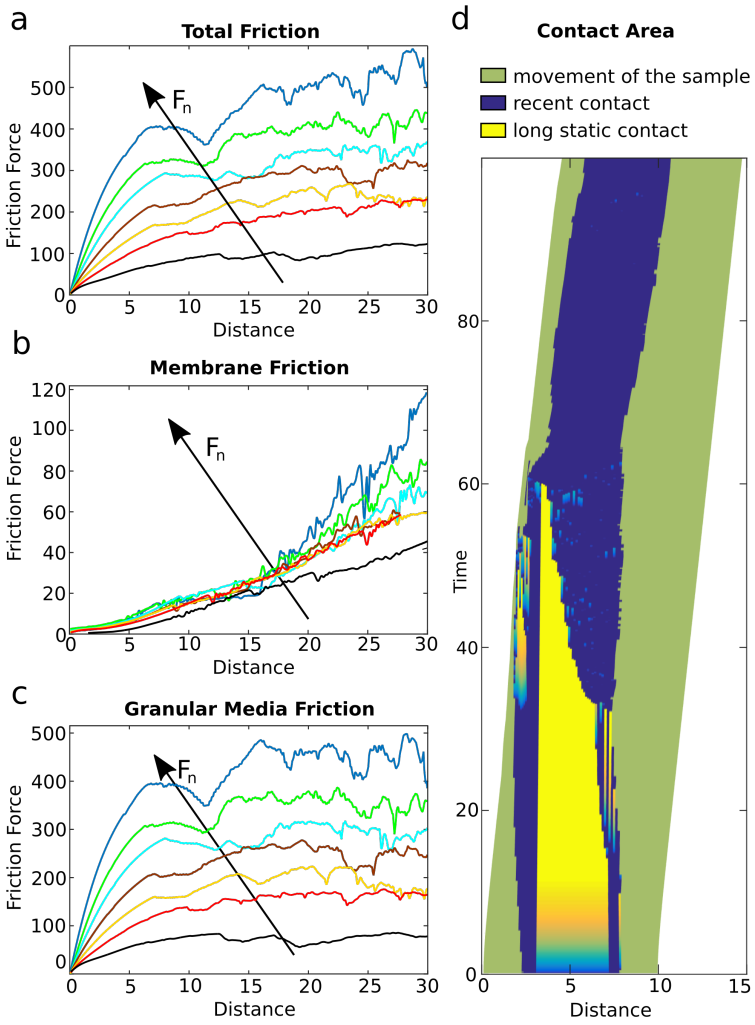


Figure 3.5: Numerical simulation of the granular friction pad. **a-c)** Friction forces in dependence of normal load $F_n$: (a) Total friction force of the sample, (b) friction force generated by membrane deformation, (c) friction force generated by the granular media. **d)** Visualization of the GMFP's contact area: The outer green area represents movement of the whole sample, the dark blue center area represents the contact area between sample and substrate, and the center transition from blue to yellow shows time-dependent adhesion of the membrane in contact with the substrate.

sliding starts at t=0, only the outer regions of the GMFP in contact move on the substrate. This can also be seen in the supplementary Videos S2-S5 of the physical sliding experiments, where the sample deforms while the contact area remains static, as well as in the simulation in figure 3.5d. The contact area stays on the same position while the overall sample moves sideways. Due to the deformation of the membrane, the static contact area grows smaller at the

forefront of the sliding until eventually global sliding sets in (yellow area completely vanishes). In contrast to bulk materials such as the investigated flat and spherical samples, the GMFP can remain in static contact for a very long time. Where other samples would already start with dynamic sliding, the GMFP still remains in static contact. While figure 3.5d is plotted for the second lowest normal force plotted in figures 3.5a-c, this behavior could be seen for all normal forces.

By using particle image velocimetry [67, 68], the same behavior could also be shown in the physical sample (see supplementary Video_S6).

## 3.2 Membrane and Filling Capacity Variations

To investigate the effect of stiffness on the granular media friction pad for contact formation as well as for friction performance, we varied filling capacity, membrane modulus and membrane thickness individually.

To be able to both see the maximum contact area on a smooth substrate as well as demonstrate the GMFP's ability to adapt to large substrate asperities, we visualized the contact area of the GMFP in static contact with a glass substrate. A 2.5mm diameter glass sphere, which resembles the contamination of the gravel particles of 1-2mm particle size for the dynamic friction experiments, was put between GMFP and substrate and the pad was loaded with eight different normal loads. The contact area lights up by total internal reflection. In the resulting pictures, the glass sphere is marked by a red dot.

The dynamic friction coefficient was measured by pulling the sample over all three substrates (flat, structured and contaminated) at four different normal loads.

### 3.2.1 Filling Capacity

By varying the filling capacity, we can change the elasticity of the GMFP. With less granular media inside, the GMFP becomes floppy and can easily adapt to the substrate. When the GMFP is filled more densely, an increase in pressure inside the granular media due to the stretching of the encasing membrane could result in higher energy dissipation from an earlier jamming transition at lower normal loads. While previously the granular pad was filled with 1.7g of

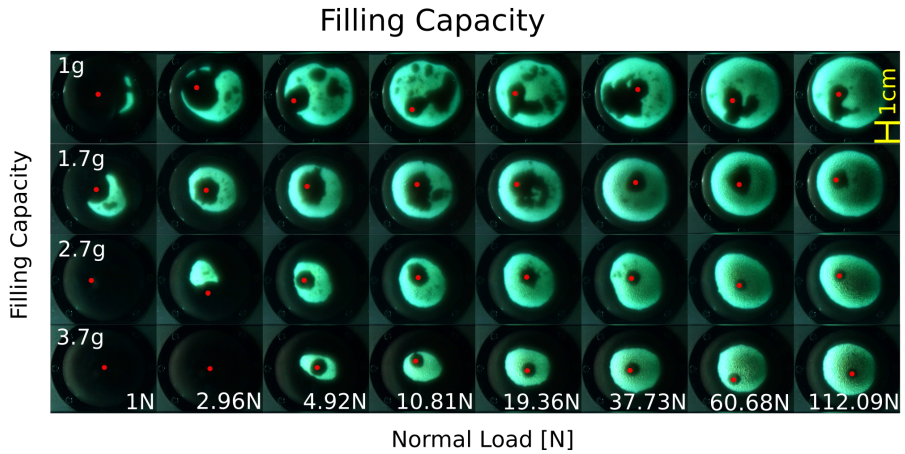


Figure 3.6: Variation of the filling capacity of the granular media friction pad: Visualization of the contact area on a glass sphere and smooth glass substrate.

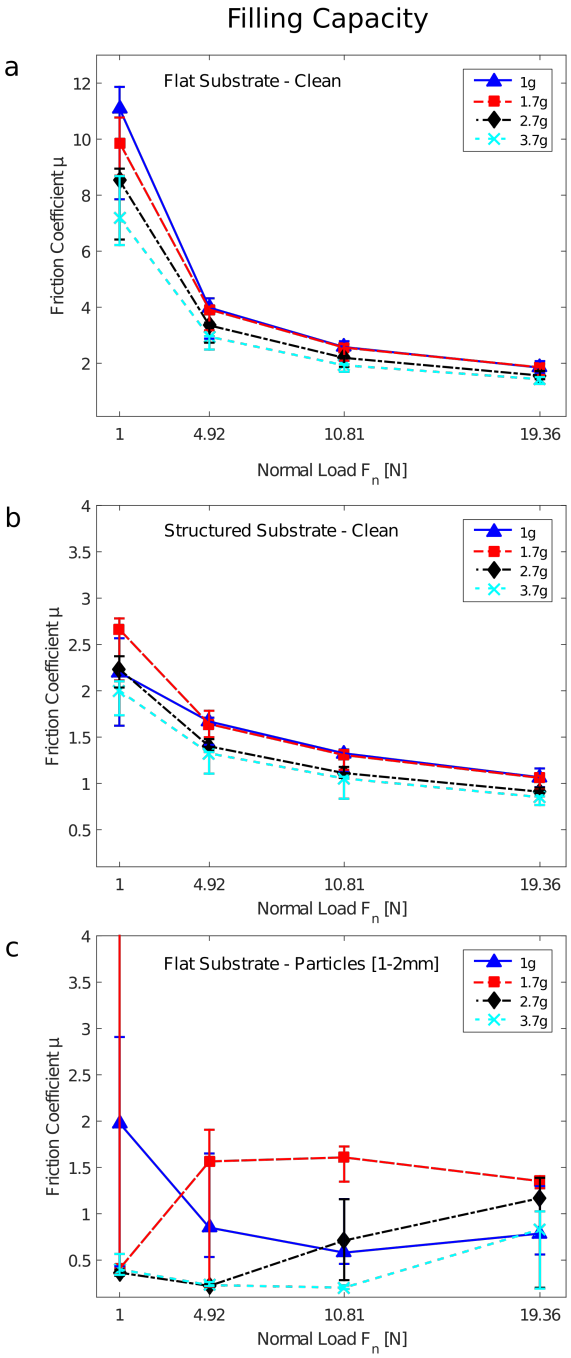


Figure 3.7: Variation of the filling capacity of the granular media friction pad. **a-c)** Friction coefficient of the differently filled granular friction pad at different normal loads $F_n$: (a) on a flat substrate, (b) on a rough/structured substrate, (c) on a flat substrate contaminated by 1-2mm large particles.

ground coffee, we now examine four different capacities ranging from 1g up to 3.7g of granular material.

The resulting static contact areas for the different filling capacities can be seen in figure 3.6. For higher filling capacities, higher normal loads are required for the GMFP to form around the glass sphere and to get into contact with the glass substrate. At high normal loads, all filling capacities achieve large contact areas with the substrate despite the glass sphere. However, the granular friction pads filled with 1g and 1.7g performed better than the 2.7g and 3.7g samples. The GMFP with the lowest filling capacity is only just about as high as the 2.5mm glass sphere between sample and substrate. Thus, under all loading conditions, the sample holder rests directly on the glass sphere, transferring most of the normal load. However, because of the low filling capacity, the nearly unstressed membrane can still achieve large contact areas with the glass substrate at low normal loads. For the 1.7g filling capacity, the sample is large enough that normal loads are mostly transferred through the granular media, resulting in largest contact areas overall.

The dynamic friction coefficients on the three different substrates can be seen in figure 3.7a-c. For all filling capacities, the highest friction coefficient was measured on the flat clean substrate (see figure 3.7a). Due to the smooth substrate, contact area maximizes and adhesion-mediated friction strongly contributes to the occurring friction forces, resulting in very large friction coefficients at low normal loads [40, 66]. Especially at the lower normal loads, a trend towards higher friction forces at lower filling capacities is observed owing to larger contact area. On the structured substrate (see figure 3.7b), friction forces are lower compared to the flat clean substrate. The lower filling capacities result in higher friction forces for all loading conditions. A clear difference in dynamic friction coefficients can be observed on the contaminated substrate (see figure 3.7c). The GMFP filled with only 1g of ground coffee is so flat that it sometimes collides with the contamination particles. Especially when the granular material is compacted even more at higher normal forces, the sample holder gets in direct contact with some of the larger gravel particles, resulting in lower friction force. The highly filled GMFP also achieves relatively low friction forces, since a high normal load is needed to press the pre-stretched membrane around the gravel particles on the substrate.

### 3.2.2 Membrane Modulus

While the granular material contributes to the friction forces at the beginning of the pulling, the deformation of the membrane significantly adds to the friction forces during the rest of the sliding motion. A stiffer membrane compresses

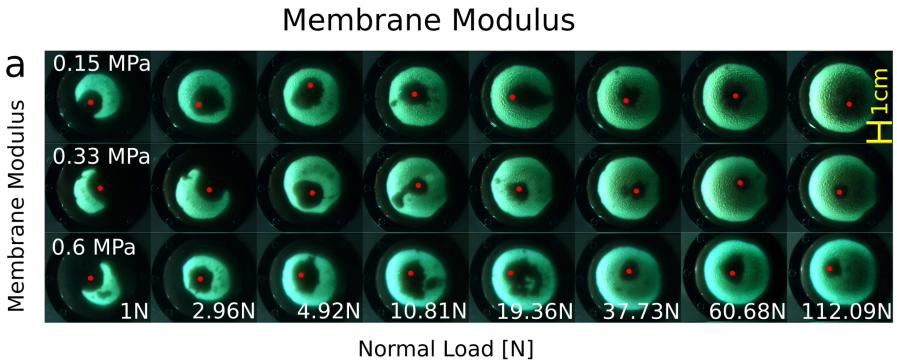


Figure 3.8: Variation of the membrane modulus of the granular media friction pad: Visualization of the contact area on a glass sphere and smooth glass substrate.

the granular media more strongly than a softer membrane. Thus, the GMFP with the stiffer membrane will not adapt to surface asperities as easily, which results in a reduction of contact area [69]. However, the stiffer membrane will require more energy when deformed during sliding. Here we use silicone rubber with three different Young's moduli of $(0.16 \pm 0.01)$MPa, $(0.33 \pm 0.01)$MPa and $(0.53 \pm 0.02)$MPa.

While the different elastic moduli strongly influence how the materials feel when manually handling them, the difference in static contact area for the different membrane moduli is very small (see figure 3.8). Only the softest $(0.16 \pm 0.01)$MPa sample shows a slightly larger contact area at lower normal loads due to its higher flexibility.

In the dynamic friction experiments, highest friction forces were always observed on the flat clean substrate (see figure 3.9a). Interestingly, the stiffer the membrane, i.e. the higher the elastic modulus, the better the friction performance. Since the contact areas for all moduli are very similar, the difference in friction performance results from higher energy dissipation in stiffer membranes during their deformation when sliding over the substrate. At higher normal loads, the softest membrane ruptures and completely fails. Thus, a stiffer membrane is preferable, since contact formation and friction performance are similar, but the stiffer membranes are more resistant to failure. Under low normal loads, the stiffest membrane performed best on the flat clean substrate. However, having an even softer membrane results in higher adaptability to substrate asperities, which can not only be seen in figure 3.8 for the low normal forces, but also on the structured and the contaminated substrates (see figures 3.9b and 3.9c). Here, the softer samples reach higher friction forces by coming into contact with the substrate despite the particle contamination.

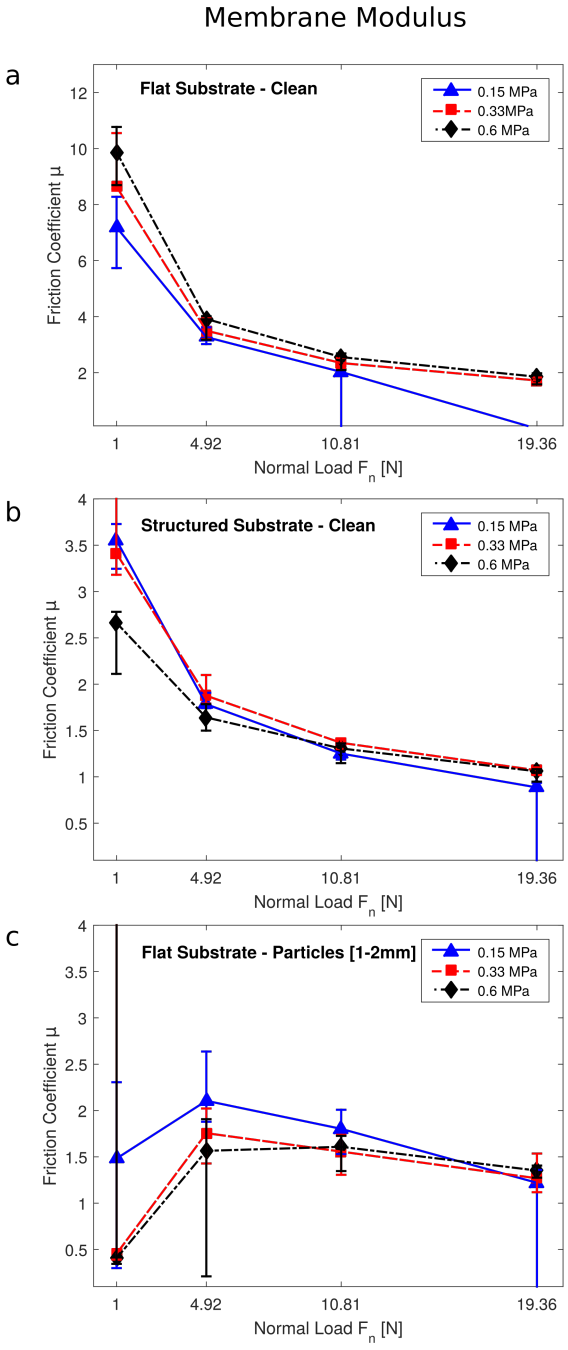


Figure 3.9: Variation of the membrane modulus of the granular media friction pad: **a-c)** Friction coefficient of the samples at different normal loads $F_n$: (a) on a flat substrate, (b) on a rough/structured substrate, (c) on a flat substrate contaminated by 1-2mm large particles.

### 3.2.3 Membrane Thickness

The stiffness of a GMFP's membrane can not only be modified by changing its elastic modulus, but also by changing its thickness. Since the membrane thickness increases the membrane's stiffness by the power of three instead of linearly like the modulus (see equation 1.1), a much more noticeable change in friction properties is expected. While the membrane thickness for the other tests was always 0.45mm, here we also investigated thicknesses of 0.15mm, 1mm and 2mm.

The change in membrane stiffness results in a big difference for the static contact area, as can be seen in figure 3.10.

For the low loading conditions, the thinnest membrane achieves the largest contact area with the substrate. The thicker membranes need much higher loading forces to be pushed around the glass bead. Thus, for a high robustness against contamination at low normal forces, a more flexible membrane is beneficial to facilitate the flowing of the granular particles.

A similar effect can be seen for the dynamic friction experiments (see figures 3.11a-c). On the clean flat substrate, the granular media friction pad does not have to deform much to achieve large contact areas (see figure 3.11a). Friction coefficients of the different membrane thicknesses are very close, with the thicker membranes achieving slightly higher friction coefficients at higher loading forces $F_n$. On the clean structured substrate (see figure 3.11b), a difference

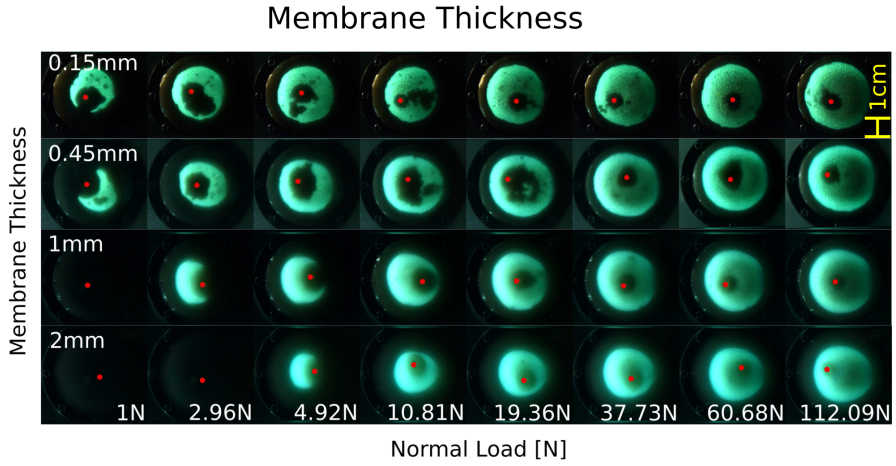


Figure 3.10: Variation of the membrane thickness of the granular media friction pad: Visualization of the contact area on a glass sphere and smooth glass substrate.

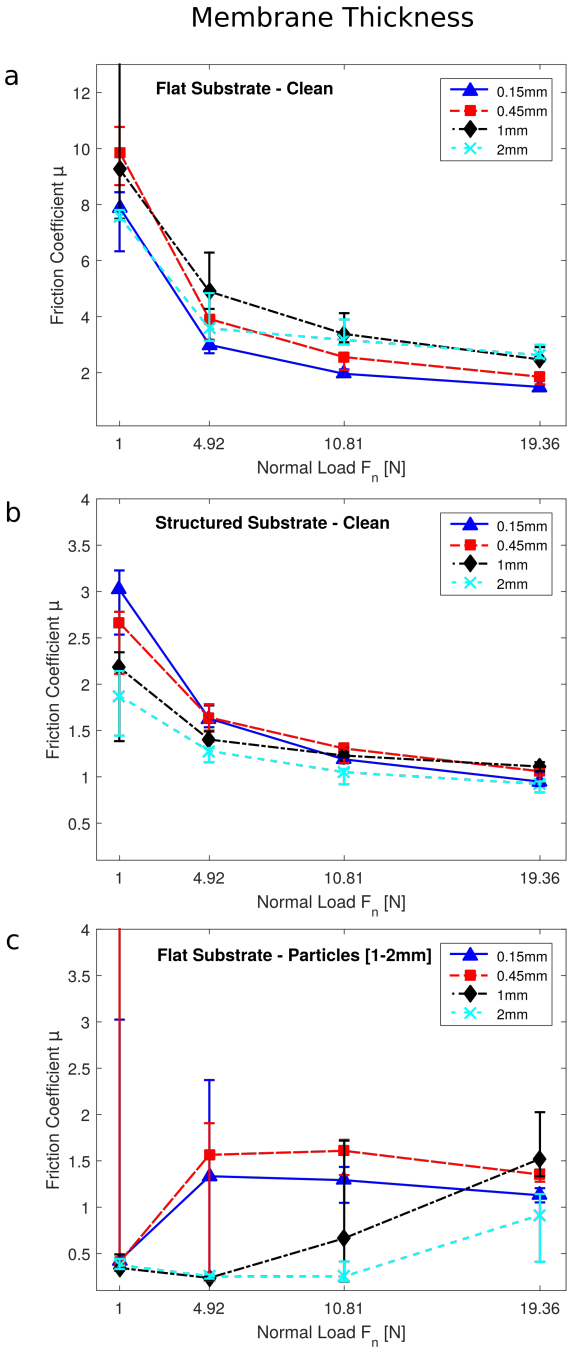


Figure 3.11: Variation of the membrane thickness of the granular media friction pad: **a-c)** Friction coefficient of the samples at different normal loads $F_n$: (a) on a flat substrate, (b) on a rough/structured substrate, (c) on a flat substrate contaminated by 1-2mm large particles.

in friction coefficients can be seen at low normal loads. The thicker membranes do not adapt easily enough to create high friction forces at these low normal loads. Only at higher normal loads, similar friction forces as with a thinner membrane can be achieved. The largest differences between the four membrane thicknesses can be seen on the flat substrate contaminated with particles (see figure 3.11c). Due to the random distribution of the contaminating particles, even at low normal loads the thinner membranes can sometimes conform around the particles and still achieve contact with the substrate during sliding, resulting in high friction forces. The thicker membranes are not flexible enough and only achieve contact at higher normal forces. The concept of the granular friction pad even works with the thickest 2mm membrane, which is able to adapt around the particles and come into contact with the substrate, but only at high normal forces.

## 3.3 Hexagon Structuring

The friction performance of the GMFP with smooth and hexagon structured membrane on dry substrate and submerged in mineral oil is illustrated in boxplots showing the average pulling force (see figure 3.12) and the resulting friction coefficient $\mu$ (see figure 3.13). The average friction coefficients of all sample and substrate combinations for the four applied normal loads are shown in table 3.1. For all normal loads, the different GMFP membranes as well as the contamination of the substrate led to a significant difference of the friction coefficient (Kruskal-Wallis rank sum test, Holm FWER method).

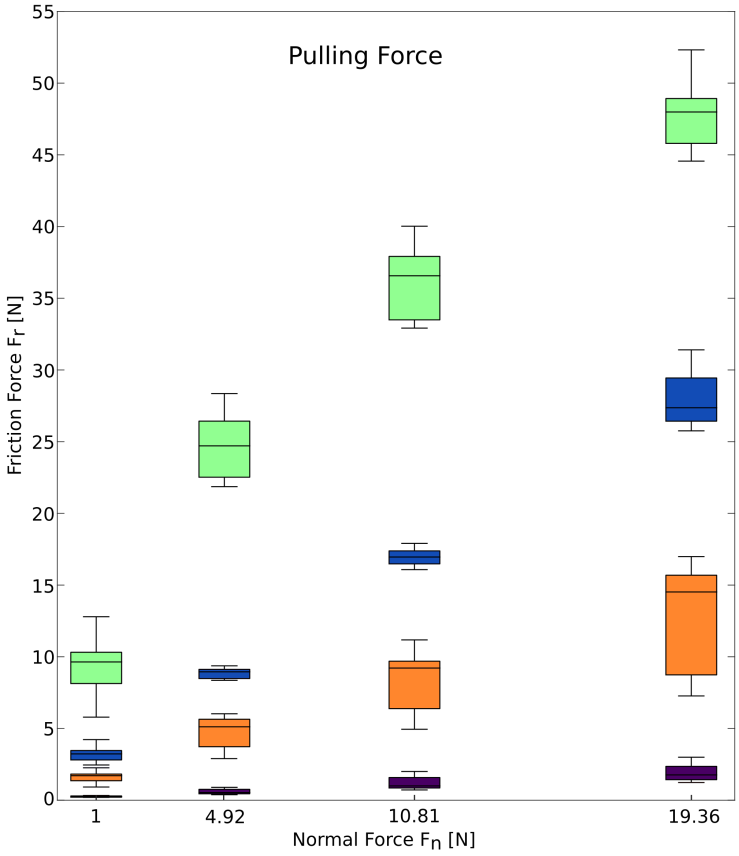


Figure 3.12: Measured pulling forces of the smooth and hexagon GMFP on dry and oily substrate. The boxes display the median and 25 and 75 percentiles with the whiskers indicating the most extreme data points.

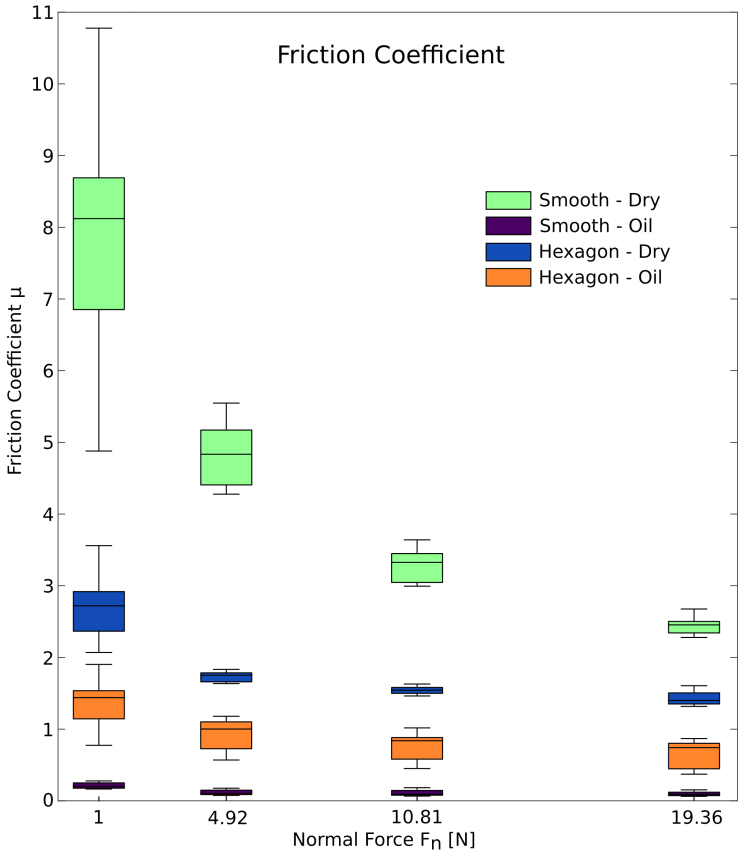


Figure 3.13: Resulting friction coefficients of the smooth and hexagon GMFP on dry and oily substrate. The boxes display the median and 25 and 75 percentiles with the whiskers indicating the most extreme data points.

### 3.3.1 Dry Substrate

On the dry substrate, the GMFP with a smooth membrane performs much better than the hexagon patterned sample. The smooth GMFP achieves extremely high friction forces at low normal load with the highest friction coefficient being $\mu = 7.9 \pm 1.5$ at the lowest normal load of 1N. At the highest normal load of 19.36N, the sample (4cm diameter) achieves friction forces up to 52N.

Hexagonal structuring leads to a significant reduction in friction forces on the dry substrate. The friction coefficient is still between $\mu = 1.4 - 2.7$ for all loading conditions examined, but generated friction forces are only about half compared to the smooth membrane.

The better friction performance of the smooth GMFP results from the larger contact area [40, 41, 66] in contrast to the grooved pattern of the hexagon mem-

brane. In addition, the deformation of the hexagon pillars during sliding could reduce the occurring friction forces by decreasing contact area even further [32, 70–72]. However, for structured and microstructured surfaces, a reduction in uncontrolled stick-slip friction is expected [14, 73].

### 3.3.2 Oily Substrate

While the smooth GMFP performed better on the dry substrate than the hexagon GMFP, the opposite is the case when submerged in mineral oil. Here, the smooth GMFP is only able to create a maximum of 3N friction force under any loading condition with the friction coefficient $\mu$ ranging from 0.1 to 0.2. In contrast, the hexagonal patterned GMFP still achieves high friction forces with a friction coefficient of $\mu = 0.7 - 1.4$. This means that while the smooth GMFP is in the same range of lubricated metals sliding [74], the hexagon structured GMFP far exceeds those values.

Submerged in oil, the lubrication never breaks down for the smooth membrane, resulting in extremely low friction coefficients. For the hexagon GMFP however, a breakdown of the lubrication film and high friction forces occur. The drainage channels between the hexagonal pillars have to be large enough for draining the lubricant depending on the viscosity of the lubricating fluid [13, 14], the cross-section of the channels [13, 14] and the sliding velocity [20, 75] while still maintaining a pillar size sufficient for large contact areas. In the case of the GMFP, the deformation of the thin elastic membrane under normal load and also from stretching during sliding results in different channel geometries depending on substrate, loading condition and occurring friction forces. The bending of the hexagonal pillars [32, 70–72] reducing the contact area during sliding has to be considered as well.

| | smooth | | hexagon | |
|---|---|---|---|---|
| $F_n$ [N] | dry | oil | dry | oil |
| 1 | $7.9 \pm 1.5$ | $0.2 \pm 0.1$ | $2.7 \pm 0.4$ | $1.4 \pm 0.3$ |
| 4.92 | $4.8 \pm 0.4$ | $0.1 \pm 0.1$ | $1.7 \pm 0.1$ | $0.9 \pm 0.2$ |
| 10.81 | $3.3 \pm 0.2$ | $0.1 \pm 0.1$ | $1.5 \pm 0.1$ | $0.8 \pm 0.2$ |
| 19.36 | $2.5 \pm 0.1$ | $0.1 \pm 0.1$ | $1.4 \pm 0.1$ | $0.7 \pm 0.2$ |

Table 3.1: Average friction coefficients with standard deviation of the smooth and hexagon GMFP on dry substrate and when completely submerged under mineral oil for all normal loads.

# Chapter 4

# Conclusion & Outlook

To summarize, we introduced a granular media friction pad (GMFP), consisting of granular media encased by an elastic membrane, that shows high friction forces on a large variety of substrates. Under low normal load, it behaves as a fluid-like material which can greatly adapt to the substrate geometry, thus creating large contact areas. Under high normal load, the GMFP undergoes the jamming transition and becomes solid-like. Here, the energy dissipation by inter-particle friction and membrane deformation leads to high friction forces during pulling along all substrates and under varying normal loads. Even on substrates covered by 1-2mm particles, the GMFP is able to create large contact areas and shows a robust design against stick and slip, since strong deformation has to occur before global slipping starts. A numerical simulation confirms these experimental findings and clearly shows the interplay between granular material and membrane for creating friction.

Furthermore, we investigated the stiffness dependence of the GMFP on the friction coefficient by varying filling capacity, membrane modulus and membrane thickness. We could show that the amount of granular media inside the GMFP is extremely important for contact formation since an excessive filling capacity, hindering unjammed motion without load, greatly reduces adaptability to substrate asperities. However, the filling capacity has to be sufficient to be able to compensate for the highest substrate asperities of the substrate. At higher normal loads, the difference in filling capacity becomes less apparent and only facilitates friction on strongly contaminated substrates. A higher pressure inside the granular media due to high filling capacity and the resulting stretching of the membrane does not outweigh the loss in contact formation and resulting adhesion-mediated friction at all loading conditions.

Membrane elasticity shows to be an equally important criterium for maximizing friction. While the effect of changing the membrane modulus is less

pronounced on both contact area and friction coefficient, although a more stiffer and durable material is to be favored, a change in membrane thickness greatly modifies the properties of the GMFP. By using a thicker membrane, more energy is needed for the deformation during sliding. However, at low normal forces, on the structured and especially on the contaminated substrate, a soft and thin membrane results in much higher friction forces.

Finally, we investigated the effect of adding hexagonal structuring to the GMFP membrane for increased resistance against wet surfaces. While the structuring results in a reduction of friction forces on dry substrates, the friction performance when submerged in mineral oil is much better than with a smooth membrane. The reduction in friction force of the hexagon GMFP on dry substrate can be explained by the smaller contact area as well as by the smaller tangential contact stiffness of the hexagonal pillars. Submerged in oil, the smooth GMFP cannot achieve high friction forces, and lubricated sliding is observed for the entire pulling distance. For the structured GMFP, the hexagonal patterning acts as drainage channels, dissipating the oil from the contact area, resulting in high friction forces throughout sliding. Thus, depending on the use case, structuring the elastic membrane of the GMFP can be extremely beneficial for overall friction performance. The small reduction in friction forces on dry substrates is outweighed by the advantages under wet conditions where the smooth GMFP completely fails.

Overall, the ability to create high friction on unknown substrate geometries makes the granular media friction pad suitable for a variety of use cases where stable grip on substrates is important. As we could show here, depending on the range of environments, expected loading forces and other external parameters, the GMFP can be optimized to achieve high friction forces throughout.

For the investigated normal loads and substrates, the reference GMFP seems to be very close to the optimum in dry conditions. In wet conditions, the reference GMFP profits greatly from the hexagon structured membrane. A further optimization of friction forces could be considered by taking the sliding direction of the hexagon GMFP into account. In our experiment, all hexagon GMFP were tested in the same orientation, i.e. with the side of the hexagons facing the sliding direction. In [15] an increase of up to 20% in friction force was observed when sliding with the hexagon tips forward. Even higher geometry dependent anisotropies were observed for elongated pillar shapes due to drainage flow and a change in tangential contact stiffness [14, 33]. This effect could be especially beneficial for an adapted hexagon GMFP when the sliding direction is predictable or friction anisotropy is desired.

Depending on environment and use case, the GMFP offers many opportunities for other modifications to further improve friction performance. For

example, different granular materials increasing energy dissipation during sliding while still being fluid-like could be explored. To prevent total failure of the GMFP, introducing nonuniform membrane thicknesses against crack propagation [76, 77] might stop the spreading of defects in the silicone membrane that result from high forces or sliding. Mimicking the complex superstructure seen in animal toe pads [13, 17, 21, 23, 26, 27], a pillar-like support system embedded in the granular media could help to bear increased forces as well as additionally fortify the GMFP against rupturing and total failure.

As is the case with its biological inspiration, the GMFP employs a system that is extremely soft and flexible when making contact with a substrate, but can create high friction forces due to its rigidification when under load and sliding. The GMFP is passive and requires no control at all, it features easy lift off the substrate after unloading since no pressure difference has to be eliminated [55] and shows high damping properties [52, 56]. This system can now be employed in a variety of technical applications where stable grip on substrates is important, and it can easily be further modified when necessary. For example, the GMFP could be very useful in robotic applications, and especially walking robots [78, 79] could profit immensely from GMFP feet. Here, the passive properties of the GMFP would result in a more stable grip during locomotion without requiring higher computational costs [80, 81], since the jamming transition resulting in the high friction forces when loaded is induced by the robot's weight only.

# Bibliography

[1] Gorb, Stanislav N. "Biological Attachment Devices: Exploring Nature's Diversity for Biomimetics." *Philosophical Transactions of the Royal Society A: Mathematical, Physical and Engineering Sciences* 366.1870 (2008): 1557-1574.

[2] Scherge, Matthias, and Stanislav N. Gorb. *Biological Micro- and Nanotribology.* Berlin: Springer Science & Business Media, 2001.

[3] Gorb, Stanislav N. "Evolution of the Dragonfly Head-Arresting System." *Proceedings of the Royal Society of London. Series B: Biological Sciences* 266.1418 (1999): 525-535.

[4] Gorb, Stanislav N., and P. J. Perez Goodwyn. "Wing-Locking Mechanisms in Aquatic Heteroptera." *Journal of Morphology* 257.2 (2003): 127-146.

[5] Petersen, Dennis S., et al. "Holding Tight to Feathers – Structural Specializations and Attachment Properties of the Avian Ectoparasite Crataerina pallida (Diptera, Hippoboscidae)." *Journal of Experimental Biology* 221.13 (2018): jeb179242.

[6] Gorb, Stanislav N. "Uncovering Insect Stickiness: Structure and Properties of Hairy Attachment Devices." *American Entomologist* 51.1 (2005): 31-35.

[7] Song, Yi, et al. "The Synergy between the Insect-Inspired Claws and Adhesive Pads Increases the Attachment Ability on Various Rough Surfaces." *Scientific Reports* 6 (2016): 26219.

[8] Haas, Fabian, and Stanislav N. Gorb. "Evolution of Locomotory Attachment Pads in the Dermaptera (Insecta)." *Arthropod Structure & Development* 33.1 (2004): 45-66.

[9] Marvi, Hamidreza, and David L. Hu. "Friction Enhancement in Concertina Locomotion of Snakes." *Journal of the Royal Society Interface* 9.76 (2012): 3067-3080.

[10] Tramsen, Halvor T., et al. "Inversion of Friction Anisotropy in a Bio-Inspired Asymmetrically Structured Surface." *Journal of The Royal Society Interface* 15.138 (2018): 20170629.

[11] Hazel, John L., et al. "Nanoscale Design of Snake Skin for Reptation Locomotions via Friction Anisotropy." *Journal of Biomechanics* 32.5 (1999): 477-484.

[12] Baum, Martina J., et al. "Anisotropic Friction of the Ventral Scales in the Snake Lampropeltis getula californiae." *Tribology Letters* 54.2 (2014): 139-150.

[13] Federle, W., et al. "Wet but not Slippery: Boundary Friction in Tree Frog Adhesive Toe Pads." *Journal of the Royal Society Interface* 3.10 (2006): 689-697.

[14] Varenberg, Michael, and Stanislav N. Gorb. "Hexagonal Surface Micropattern for Dry and Wet Friction." *Advanced Materials* 21.4 (2009): 483-486.

[15] Chen, Huawei, et al. "Bioinspired Surface for Surgical Graspers Based on the Strong Wet Friction of Tree Frog Toe Pads." *ACS Applied Materials & Interfaces* 7.25 (2015): 13987-13995.

[16] Barnes, W. Jon P., et al. "Elastic Modulus of Tree Frog Adhesive Toe Pads." *Journal of Comparative Physiology* A 197.10 (2011): 969-978.

[17] Gorb, Stanislav N., and Matthias Scherge. "Biological Microtribology: Anisotropy in Frictional Forces of Orthopteran Attachment Pads Reflects the Ultrastructure of a Highly Deformable Material." *Proceedings of the Royal Society of London. Series B: Biological Sciences* 267.1449 (2000): 1239-1244.

[18] Büscher, Thies H., et al. "The Evolution of Tarsal Adhesive Microstructures in Stick and Leaf Insects (Phasmatodea)." *Frontiers in Ecology and Evolution* 6.69 (2018).

[19] Green, David M., and Pere Alberch. "Interdigital Webbing and Skin Morphology in the Neotropical Salamander Genus Bolitoglossa (Amphibia; Plethodontidae)." *Journal of Morphology* 170.3 (1981): 273-282.

[20] Huang, Wei, and Xiaolei Wang. "Biomimetic Design of Elastomer Surface Pattern for Friction Control under Wet Conditions." *Bioinspiration & Biomimetics* 8.4 (2013): 046001.

[21] Barnes, W. Jon P. "Functional Morphology and Design Constraints of Smooth Adhesive Pads." *MRS Bulletin* 32.6 (2007): 479-485.

[22] Kosaki, A., and R. Yamaoka. "Chemical Composition of Footprints and Cuticula Lipids of three Species of Lady Beetles." *Japanese Journal of Applied Entomology and Zoology* 40 (1996): 47-53.

[23] Gorb, Stanislav N., Yuekan Jiao, and Matthias Scherge. "Ultrastructural Architecture and Mechanical Properties of Attachment Pads in Tettigonia viridissima (Orthoptera Tettigoniidae)." *Journal of Comparative Physiology A* 186.9 (2000): 821-831.

[24] Federle, Walter, and Thomas Endlein. "Locomotion and Adhesion: Dynamic Control of Adhesive Surface Contact in Ants." *Arthropod Structure & Development* 33.1 (2004): 67-75.

[25] Federle, Walter, et al. "Biomechanics of the Movable Pretarsal Adhesive Organ in Ants and Bees." *Proceedings of the National Academy of Sciences* 98.11 (2001): 6215-6220.

[26] Jiao, Yuekan, Stanislav N. Gorb, and Matthias Scherge. "Adhesion Measured on the Attachment Pads of Tettigonia viridissima (Orthoptera, Insecta)." *Journal of Experimental Biology* 203.12 (2000): 1887-1895.

[27] Peressadko, A. G., N. Hosoda, and B. N. J. Persson. "Influence of Surface Roughness on Adhesion between Elastic Bodies." *Physical Review Letters* 95.12 (2005): 124301.

[28] Unver, Ozgur, et al. "Geckobot: a Gecko Inspired Climbing Robot Using Elastomer Adhesives." *Proceedings 2006 IEEE International Conference on Robotics and Automation, 2006.* IEEE, 2006.

[29] Daltorio, Kathryn A., et al. "A Small Wall-Walking Robot with Compliant, Adhesive Feet." *2005 IEEE/RSJ International Conference on Intelligent Robots and Systems.* IEEE, 2005.

[30] Asbeck, Alan T., et al. "Scaling Hard Vertical Surfaces with Compliant Microspine Arrays." *The International Journal of Robotics Research* 25.12 (2006): 1165-1179.

[31] Spenko, Matthew J., et al. "Biologically Inspired Climbing with a Hexapedal Robot." *Journal of Field Robotics* 25.4-5 (2008): 223-242.

[32] Drotlef, Dirk-Michael, et al. "Insights into the Adhesive Mechanisms of Tree Frogs Using Artificial Mimics." *Advanced Functional Materials* 23.9 (2013): 1137-1146.

[33] Rand, Charles J., and Alfred J. Crosby. "Friction of Soft Elastomeric Wrinkled Surfaces." *Journal of Applied Physics* 106.6 (2009): 064913.

[34] Barnes, W. Jon P. "Tree Frogs and Tire Technology." *Tire Technology International* 99 (1999): 42-47.

[35] Barnes, W. Jon P., et al. "Bionics and Wet Grip." *Tire Technology International* 2002 (2002): 56-60.

[36] Persson, Bo N. J. "Wet Adhesion with Application to Tree Frog Adhesive Toe Pads and Tires." *Journal of Physics: Condensed Matter* 19.37 (2007): 376110.

[37] Persson, Bo N. J. "Theory of Rubber Friction and Contact Mechanics." *The Journal of Chemical Physics* 115.8 (2001): 3840-3861.

[38] Brown, Eric, et al. "Universal Robotic Gripper Based on the Jamming of Granular Material." *Proceedings of the National Academy of Sciences* 107.44 (2010): 18809-18814.

[39] Jaeger, Heinrich M., Sidney R. Nagel, and Robert P. Behringer. "Granular Solids, Liquids, and Gases." *Reviews of Modern Physics* 68.4 (1996): 1259-1273.

[40] Persson, Bo N. J. "Silicone Rubber Adhesion and Sliding Friction." *Tribology Letters* 62.2 (2016): 34.

[41] Popov, Valentin L. *Contact Mechanics and Friction.* Berlin: Springer, 2010.

[42] Jaeger, Heinrich M. "Celebrating Soft Matter's 10th Anniversary: Toward Jamming by Design." *Soft Matter* 11.1 (2015): 12-27.

[43] Majmudar, T. S., et al. "Jamming Transition in Granular Systems." *Physical Review Letters* 98.5 (2007): 058001.

[44] Cates, M. E., et al. "Jamming, Force Chains, and Fragile Matter." *Physical Review Letters* 81.9 (1998): 1841.

[45] Miller, Brian, Corey O'Hern, and R. P. Behringer. "Stress Fluctuations for Continuously Sheared Granular Materials." *Physical Review Letters* 77.15 (1996): 3110.

[46] Albert, Istvan, et al. "Granular Drag on a Discrete Object: Shape Effects on Jamming." *Physical Review E* 64.6 (2001): 061303.

[47] Forterre, Yoël, and Olivier Pouliquen. "Flows of Dense Granular Media." *Annual Review of Fluid Mechanics* 40 (2008): 1-24.

[48] Bi, Dapeng, et al. "Jamming by Shear." *Nature* 480.7377 (2011): 355.

[49] Corwin, Eric I., Heinrich M. Jaeger, and Sidney R. Nagel. "Structural Signature of Jamming in Granular Media." *Nature* 435.7045 (2005): 1075.

[50] Tiwari, Avinash, et al. "Rubber Contact Mechanics: Adhesion, Friction and Leakage of Seals." *Soft Matter* 13.48 (2017): 9103-9121.

[51] Myshkin, N. K., M. I. Petrokovets, and A. V. Kovalev. "Tribology of Polymers: Adhesion, Friction, Wear, and Mass-Transfer." *Tribology International* 38.11-12 (2005): 910-921.

[52] Najmuddin, Ahmad, Yasuhiro Fukuoka, and Shota Ochiai. "Experimental Development of Stiffness Adjustable Foot Sole for Use by Bipedal Robots Walking on Uneven Terrain." *2012 IEEE/SICE International Symposium on System Integration (SII)*, IEEE, 2012.

[53] Hauser, Simon, et al. "Fast State-Switching of a Jamming-Based Foot." *The 8th International Symposium on Adaptive Motion of Animals and Machines* (2017): 41-42.

[54] Hauser, Simon, et al. "Compliant Universal Grippers as Adaptive Feet in Legged Robots." *Advanced Robotics* 32.15 (2018): 825-836.

[55] Amend, John R., et al. "A Positive Pressure Universal Gripper Based on the Jamming of Granular Material." *IEEE Transactions on Robotics* 28.2 (2012): 341-350.

[56] Hauser, Simon, et al. "Friction and Damping of a Compliant Foot Based on Granular Jamming for Legged Robots." *2016 6th IEEE International Conference on Biomedical Robotics and Biomechatronics (BioRob).* IEEE, 2016.

[57] Cheng, Nadia G., et al. "Design and Analysis of a Robust, Low-Cost, Highly Articulated Manipulator Enabled by Jamming of Granular Media." *2012 IEEE International Conference on Robotics and Automation.* IEEE, 2012.

[58] Murphy, Kieran A., et al. "Freestanding Loadbearing Structures with Z-Shaped Particles." *Granular Matter* 18.2 (2016): 26.

[59] Steltz, Erik, et al. "Jsel: Jamming Skin Enabled Locomotion." *2009 IEEE/RSJ International Conference on Intelligent Robots and Systems.* IEEE, 2009.

[60] Athanassiadis, Athanasios G., et al. "Particle Shape Effects on the Stress Response of Granular Packings." *Soft Matter* 10.1 (2014): 48-59.

[61] Loeve, Arjo J., et al. "Vacuum Packed Particles as Flexible Endoscope Guides with Controllable Rigidity." *Granular Matter* 12.6 (2010): 543-554.

[62] Jiang, Allen, et al. "Robotic Granular Jamming: Does the Membrane Matter?." *Soft Robotics* 1.3 (2014): 192-201.

[63] Persson, Bo N. J., et al. "Rubber Friction on Wet and Dry Road Surfaces: The Sealing Effect." *Physical Review B* 71.3 (2005): 035428.

[64] Roberts, A. D. "Squeeze Films between Rubber and Glass." *Journal of Physics D: Applied Physics* 4.3 (1971): 423.

[65] Liu, Andrea J., and Sidney R. Nagel. "Nonlinear Dynamics: Jamming is Not Just Cool Any More." *Nature* 396.6706 (1998): 21.

[66] Heise, Rainer, and Valentin L. Popov. "Adhesive Contribution to the Coefficient of Friction between Rough Surfaces." *Tribology Letters* 39.3 (2010): 247-250.

[67] Thielicke, William, and Eize Stamhuis. "PIVlab – Towards User-Friendly, Affordable and Accurate Digital Particle Image Velocimetry in MATLAB." *Journal of Open Research Software* 2.1 (2014).

[68] Thielicke, William. *The Flapping Flight of Birds: Analysis and Application.* Groningen: U of Groningen, 2014.

[69] Amend, John, et al. "Soft Robotics Commercialization: Jamming Grippers from Research to Product." *Soft Robotics* 3.4 (2016): 213-222.

[70] Murarash, Boris, Yan Itovich, and Michael Varenberg. "Tuning Elastomer Friction by Hexagonal Surface Patterning." *Soft Matter* 7.12 (2011): 5553-5557.

[71] Varenberg, Michael, and Stanislav N. Gorb. "Shearing of Fibrillar Adhesive Microstructure: Friction and Shear-Related Changes in Pull-Off Force." *Journal of The Royal Society Interface* 4.15 (2007): 721-725.

[72] Varenberg, Michael, and Stanislav N. Gorb. "Close-Up of Mushroom-Shaped Fibrillar Adhesive Microstructure: Contact Element Behaviour." *Journal of the Royal Society interface* 5.24 (2007): 785-789.

[73] Kligerman, Yuri, and Michael Varenberg. "Elimination of Stick-Slip Motion in Sliding of Split or Rough Surface." *Tribology Letters* 53.2 (2014): 395-399.

[74] Bowden, Frank Philip, and David Tabor. *The Friction and Lubrication of Solids.* Vol. 1. Oxford: Oxford UP, 2001.

[75] Hanna, Gavin, W. Jon, and W. P. Jon Barnes. "Adhesion and Detachment of the Toe Pads of Tree Frogs." *Journal of Experimental Biology* 155.1 (1991): 103-125.

[76] Rajabi, Hamed, et al. "The Probability of Wing Damage in the Dragonfly Sympetrum vulgatum (Anisoptera: Libellulidae): A Field Study." *Biology Open* 6.9 (2017): 1290-1293.

[77] Rajabi, Hamed, et al. "Wing Cross Veins: An Efficient Biomechanical Strategy to Mitigate Fatigue Failure of Insect Cuticle." *Biomechanics and Modeling in Mechanobiology* 16.6 (2017): 1947-1955.

[78] Hirai, Kazuo, et al. "The Development of Honda Humanoid Robot." *Proceedings. 1998 IEEE International Conference on Robotics and Automation.* Vol. 2. IEEE, 1998.

[79] Raibert, Marc, et al. "Bigdog, the Rough-Terrain Quadruped Robot." *IFAC Proceedings Volumes* 41.2 (2008): 10822-10825.

[80] Pfeifer, Rolf, Fumiya Iida, and Gabriel Gómez. "Morphological Computation for Adaptive Behavior and Cognition." *International Congress Series.* Vol. 1291. Elsevier, 2006.

[81] Pfeifer, Rolf, Max Lungarella, and Fumiya Iida. "Self-Organization, Embodiment, and Biologically Inspired Robotics." *Science* 318.5853 (2007): 1088-1093.

# Supplementary Information

## Video_S1

The granular media friction pad is pulled over the flat clean substrate at 1mm/s for a short distance. The contribution of the membrane's deformation to the friction force is considered negligible since no large deformation occurs compared to videos S2 - S6. Thus, the increase in the slope of the friction force when pulling starts is generated by the granular media inside the soft membrane that undergoes the jamming transition depending on the normal load.

## Video_S2

Side view of the granular media friction pad on flat substrate at a normal load of $F_n = 1$N. The granular media friction pad strongly deforms at the beginning of pulling due to the thin elastic membrane encasing the granular media.

## Video_S3

Visualization of the contact area of the granular media friction pad sliding over a glass substrate with a normal load of $F_n = 1$N. The camera looks from below through the glass substrate onto the GMFP. To visualize the contact area, the glass substrate is lit from the side. By using total internal reflection, the parts of the GMFP in contact with the glass substrate light up green, thus making the contact area visible during the whole experiment.

## Video_S4

Side view of the granular media friction pad on the flat substrate contaminated by 0.5g of 1-2mm gravel particles at a normal load of $F_n = 19.36$N. The pad conforms around the contaminating particles and reaches contact with the sub-

strate. It greatly deforms during sliding and is able to achieve high friction forces even though the contamination is about half the sample height.

## Video_S5

Visualization of the contact area of the granular media friction pad sliding over a glass substrate contaminated by 0.5g of 1-2mm gravel particles at a normal load of $F_n = 10.81$N. The camera looks from below through the glass substrate onto the GMFP. To visualize the contact area, the glass substrate is lit from the side. By using total internal reflection, the parts of the GMFP in contact with the glass substrate light up green, thus making the contact area visible during the whole experiment.

## Video_S6

Using particle image velocimetry, the deformation of the granular media friction pad while being pulled over a glass substrate is illustrated. The original video is shown on the left. Here, the outer areas of the glass substrate as well as the inside of the silicone membrane have been dotted by small paint speckles. On the right, the particle image velocimetry computes the velocity of these speckles. As long as the speckles on the membrane have the same velocity as the speckles applied to the glass substrate, static contact is observed. Similarly to the numerical simulation, parts of the sample stay in static contact with the substrate for a long time until global slipping starts.

# Acknowledgements

I would like to take this opportunity to sincerely thank my supervisor, Prof. Dr. Stanislav N. Gorb, for his trust in me. His experience and advice have not only immensely strengthened this thesis, but my scientific and personal growth as well.
I also thank Prof. Dr. Poramate Manoonpong for his support in my master thesis, which introduced me to the topic of friction and to Prof. Gorb's research group, as well as for being my second referee.
My thanks go to Prof. Dr. Kersten for acting as chairman of the examination board, and to Prof. Dr. Kuhlmann for his membership in the examination board.

I would like to express my special appreciation and thanks to Dr. Lars Heepe for the help, guidance and advice in supporting me during my work on this fascinating topic. He always has time for questions, ideas and discussions.
I am very grateful for the cooperation with Prof. Dr. Alexander E. Filippov, which has contributed significantly to the numerical description of the GMFP.
I thank Dr. Hamed Rajabi for discussions and helpful comments at any time.
Thank you to the entire research group Functional Morphology and Biomechanics at Kiel University. You have made the office a second home.

I want to thank my parents for their love and patience and for giving me the opportunity to study physics and to follow any road I set out to take.
Finally and most importantly, this work would not have been possible without my wife Ronja, whose support, encouragement and love I admire endlessly.

# Eidesstattliche Erklärung

Hiermit erkläre ich, dass die vorliegende Dissertation abgesehen von der Beratung durch den Betreuer nach Inhalt und Form meine eigene Arbeit ist und alle benutzten Quellen angegeben sind.
Diese Arbeit wurde weder ganz oder zum Teil im Rahmen eines Prüfungsverfahrens an anderer Stelle vorgelegt. Die Arbeit ist unter Einhaltung der Regeln guter wissenschaftlicher Praxis der Deutschen Forschungsgemeinschaft entstanden.
Es wurde kein akademischer Grad entzogen.

Kiel, den _____ _____

(Halvor Tram Tramsen)